Inorg. Chem. **2007**, *46*, 3467−3474

Crystal Structures of Incommensurately Modulated $Ln(PO_3)_3$ (Ln = Tb−Yb) and Commensurate $Gd(PO_3)_3$ and $Lu(PO_3)_3$

Henning A. Höppe* and Stefan J. Sedlmaier

Institut für Anorganische und Analytische Chemie, Albert-Ludwigs-Universität Freiburg, Albertstrasse 21, D-79104 Freiburg im Breisgau, Germany

Received August 24, 2006

The crystal structure of the late lanthanoids' *catena*-polyphosphates $Ln(PO_3)_3$ (Ln = Tb−Yb) is incommensurately modulated ($Dy(PO_3)_3$: space group $Cc(0\beta0)0$; $Z = 4$; $a = 1417.4(4)$, $b = 670.96(14)$, $c = 1009.5(3)$ pm; $\beta = 127.62(2)°$, $\mathbf{q} = 0.364\mathbf{b}^*$; $R_{all} = 0.057$, $wR_{all} = 0.071$; 293 K) and consists of infinite chains of corner-sharing PO_4 tetrahedra. The cations are coordinated 6-fold in an almost octahedral arrangement over the whole modulation period. All atoms comprise a sinoidal positional modulation. The basic structure can be derived from a fcc packing which explains the pseudo-face-centering observed in the diffraction patterns. The crystal structure of $Lu(PO_3)_3$ is isotypic with *C*-type phosphates (*Cc*; $Z = 12$; $a = 1397.2(1)$, $b = 2001.8(2)$, $c = 995.56(9)$ pm; $\beta = 127.351(6)°$; R1 = 0.042, wR2 = 0.097, 293 K), and $Gd(PO_3)_3$ crystallizes in a new structure type (*I*2/*a*; $Z = 16$; $a = 2601.7(2)$, $b = 1351.1(1)$, $c = 1008.4(1)$ pm; $\beta = 119.311(6)°$; R1 = 0.039, wR2 = 0.092; 293 K). Both can be described in terms of superstructures of the basic structure unit cell of the incommensurate phases, and thus, a consistent structural description of many polyphosphates is provided. $Tb(PO_3)_3$ was obtained as single phase adopting a novel synthesis under reducing conditions. The absence of an inversion center in the incommensurate phases and $Lu(PO_3)_3$ was proved by a SHG experiment. The vibrational spectra are also discussed.

1. Introduction

Crystalline compounds of rare-earth metals with condensed anions are of broad interest for optical applications, but unfortunately there is still a lack of knowledge of structural details in many condensed phosphates.[1] Therefore, it is our approach to clarify the coordination environment around the lanthanoid ions by a careful determination of their crystal structures and then to identify suitable host lattices useful for optical applications as, e.g., quantum cutting phosphors[2] or upconversion materials with, e.g., Er^{3+}.[3] The polyphosphates $Ln(PO_3)_3$ with Ln = Gd−Lu of the late rare earth metal ions have been known quite long, but up to now their crystal structures have not been described satisfactorily despite some reports on crystal structure analyses.

Although Beucher[4] synthesized all rare-earth polyphosphates, for lack of single crystals, she was unable to determine the crystal structure of the compounds. On the basis of powder diffraction data, she recognized that the series of the Ln polyphosphates is defined by so far two different structure types. This proved true with the first crystal structures of Ln polyphosphates in 1974, when Hong[5,6] described $Nd(PO_3)_3$ orthorhombic (space group $C222_1$ (No. 20)) and $Yb(PO_3)_3$ monoclinic (space group $P2_1/c$ (No. 14)). X-ray analysis with all Ln polyphosphate powders finally showed that the early rare-earth polyphosphates La−Gd crystallize orthorhombic and the late rare-earth polyphosphates Sm−Lu crystallize monoclinic.[7] While the orthorhombic $Ln(PO_3)_3$ structure type was further confirmed with the crystal structures of $La(PO_3)_3$[8] and $Pr(PO_3)_3$,[9] which are isotypic with $Nd(PO_3)_3$, the description of the monoclinic $Ln(PO_3)_3$ structure type was not consistent.[6,10,11]

* To whom correspondence should be addressed. E-mail: henning.hoeppe@ac.uni-freiburg.de. Fax: (+49) 761-203-6012.

(1) Durif, A. *Crystal Chemistry of Condensed Phosphates*; Plenum Press: New York, 1995.
(2) Ronda, C. *J. Lumin.* **2002**, *100*, 301.
(3) Witte, O.; Stolz, H., von der Osten, W. *J. Phys. D* **1996**, *29*, 561.
(4) Beucher, M. *The Rare Earth Elements*; Paris CNRS (Centre National de la Recherche Scientifique): Paris, 1970; Coll. No. 180, Vol. 1, pp 331−336.
(5) Hong, H. Y.-P. *Acta Crystallogr. B* **1974**, *30*, 468.
(6) Hong, H. Y.-P. *Acta Crystallogr. B* **1974**, *30*, 1857.
(7) Melnikov, P. P.; Komissarova, L. N.; Butuzova, T. A. *Izv. Akad. Nauk SSSR, Neorg. Mater.* **1981**, *17*, 2110.
(8) Matuszewski, J.; Kropiwnicka, J.; Znamierowska, T. *J. Solid State Chem.* **1988**, *75*, 285.
(9) Jouini, A.; Ferid, M., Gâcon, J.-C.; Grosvalet, L.; Thozet, A.; Trabelsi-Ayadi, M. *Mater. Res. Bull.* **2003**, *38*, 1613.

10.1021/ic0616030 CCC: $37.00
Published on Web 04/06/2007

A main problem may have been that part of these crystal structures is incommensurately modulated. In this work we try to elucidate the crystal structures of $Ln(PO_3)_3$ with Ln = Tb−Yb, which are incommensurately modulated, and additionally the crystal structures of $Gd(PO_3)_3$, which exhibits a new structure type, and $Lu(PO_3)_3$.

2. Experimental Section

The phosphates $Ln(PO_3)_3$ with Ln = Gd−Lu were synthesized in two different ways, i.e., first according to previous works ("classical" synthesis,[1] eq 1) starting from ammonium hydrogen phosphate and the respective lanthanoide oxide and second according to recent works on synthesizing phosphates under reducing conditions using phosphorous acid and the respective Ln_2O_3 (eq 2).[12,13] The crystallinity of the obtained samples was comparable but in the case of $Yb(PO_3)_3$ better using phosphorous acid. Furthermore, $Tb(PO_3)_3$ can only be obtained single phase by method 2 under reducing conditions to avoid Tb^{4+}-containing impurities.

Method 1. The synthesis of $Dy(PO_3)_3$ was performed according to

$$Dy_2O_3 + 6NH_4H_2PO_4 \rightarrow 2Dy(PO_3)_3 + 9H_2O + 6NH_3 \quad (1)$$

A mixture of 60.0 mg (161 μmol) of dysprosium oxide (Kristallhandel Kelpin, 99.9%) and 111 mg (965 μmol) of ammonium dihydrogen phosphate (ABCR, 98%) was transferred into an alumina crucible. The latter was then heated to 873 K with a rate of 100 K h^{-1} and maintained at this temperature for 10 h. After cooling of the sample to room temperature with a rate of 60 K h^{-1} 118 mg (295 μmol, 92%) of $Dy(PO_3)_3$ was obtained as a crystalline, colorless, and nonhygroscopic powder.

Method 2. The synthesis of $Yb(PO_3)_3$ was performed in a tube furnace according to

$$Yb_2O_3 + 10H_3PO_3 \rightarrow 2Yb(PO_3)_3 + 4P + 15H_2O \quad (2)$$

Under argon a mixture of 48.0 mg (122 μmol) of ytterbium oxide (Auer-Remy K.-G., 99.9%) and 101 mg (1.23 mmol) of phosphorous acid (Riedel-de Haën, 98%) was transferred into an alumina boat. The latter was then heated under a nitrogen flow to 1123 K with a rate of 120 K h^{-1}. After 19 h no further condensation of water and red phosphorus was detected and the mixture was cooled to room temperature with a rate of 120 K h^{-1}. To get crystalline $Yb(PO_3)_3$, the mostly amorphous product was reground and tempered at 1123 K for 24 h (heating rate, 120 K h^{-1}; cooling rate, 120 K h^{-1}). Finally 89.0 mg (217 μmol, 89%) of $Yb(PO_3)_3$ was obtained as a crystalline, colorless, and nonhygroscopic powder.

The composition of obtained samples was checked by energy dispersive X-ray spectroscopy (EDX) and confirmed the respective Ln:P ratios.

Crystal Structure Analyses of the Incommensurately Modulated Phases. X-ray diffraction data were collected on a Stoe IPDS II area detection diffractometer. The basic diffraction pattern was indexed on the basis of a *C*-centered monoclinic unit cell. According to the diffraction pattern, satellite reflections besides the normal Bragg reflections were found which could be indexed considering an incommensurate modulation vector $\mathbf{q} \approx 0.36\mathbf{b}^*$. The crystal structure of $Ln(PO_3)_3$ with Ln = Tb, Dy, Ho, Er, Tm, and Yb was solved by direct methods using SHELXS[14] and refined with anisotropic displacement parameters and positional modulation waves for all atoms using the JANA2000 package.[15] Typical parameters of the single-crystal data collections and the refinements are given in Table 1 by showing the data for $Dy(PO_3)_3$. Table 2 gives an overview about the lattice parameters and modulation vectors of the incommensurate phases. Tables 3 and 4 show the positional and displacement parameters for all atoms. The obtained crystalline products were single phase according to X-ray powder diffractometry (Figure 1). Further details of the crystal structure investigations (especially the coefficients of the modulation functions) may be obtained from the Fachinformationszentrum Karlsruhe, D-76344 Eggenstein-Leopoldshafen, Germany (e-mail: crysdata@fiz-karlsruhe.de) on quoting the depository number CSD-416844 ($Dy(PO_3)_3$), the name of the authors, and citation of this publication.

Table 1. Crystallographic Data for $Dy(PO_3)_3$

formula, fw	$Dy(PO_3)_3$, 399.42
cryst system/super space group/*Z*	monoclinic, $Cc(0\beta0)0$, 4
modulation vector	$\mathbf{q} = 0.364(2)\mathbf{b}^*$
lattice params/pm, deg	$a = 1417.4(4)$ $b = 670.96(14)$, $\beta = 127.62(2)$ $c = 1009.5(3)$
cell vol/10^6 pm^3	760.3(3)
X-ray density/g cm^{-3}	3.489
F(000)	732
abs coeff μ/mm^{-1}	10.48
diffractometer (single-cryst X-ray analysis)	Stoe IPDS area detection diffractometer II
temp/K	293(2)
cryst size/mm^3	0.06 × 0.05 × 0.04
diffractn range/radiatn	$5.3° \le 2\theta \le 60.1°$/71.073 pm (Mo K$\alpha$)
h, *k*, *l*	$h = -19 \rightarrow 19$, $k = -9 \rightarrow 9$, $l = -14 \rightarrow 14$
m	$m = -1 \rightarrow 1$
tot./indpndnt/obsd no. reflcns	22 845/6492/1868 $F_o^2 \ge 2\sigma(F_o^2)$
corrs	Lorentz, polarization, extinction
refined params	196
extinction coeff χ	0.0081(5)
Flack param (refined as inv twin)	0.26(4)
GooF	1.04
R indices (all data)	$R_{all} = 0.057$, $wR_{all} = 0.071$
R_{sat}	$R_{sat} = 0.083$, $wR_{sat} = 0.170$

Crystal Structure Analyses of $Gd(PO_3)_3$ and $Lu(PO_3)_3$. X-ray diffraction data were collected on a Stoe IPDS II area detection diffractometer. The diffraction pattern was indexed on the basis of a *C*-centered ($Lu(PO_3)_3$) and a body-centered ($Gd(PO_3)_3$) monoclinic unit cell, respectively. The crystal structures of $Lu(PO_3)_3$ and $Gd(PO_3)_3$ were solved by direct methods using SHELXTL[14] and refined with anisotropic displacement parameters for all atoms. Both data sets have been corrected for absorption by applying a numerical correction on the basis of an optimized crystal shape by the program X-Shape (Stoe & Cie, Darmstadt, Germany).

Further details of the crystal structure investigations may be obtained from the Fachinformationszentrum Karlsruhe, D-76344 Eggenstein-Leopoldshafen, Germany (e-mail: crysdata@fiz-karlsruhe.de) on quoting the depository numbers CSD-416842 ($Lu(PO_3)_3$) and CSD-416843 ($Gd(PO_3)_3$), the name of the authors, and citation of this publication.

Vibrational Spectroscopy. Infrared spectra were recorded on a Bruker IFS 66v/S spectrometer scanning a range from 400 to

(10) Dorokhova, G. I.; Karpov, O. G. *Kristallografiya* **1984**, *29*, 677.
(11) Anisimova, N. Yu.; Trunov, V. K.; Karmanovskaya, N. B.; Chudinova, N. N. *Izv. Akad. Nauk SSSR, Neorg. Mat.* **1992**, *28*, 441.
(12) Höppe, H. A. *Z. Anorg. Allg. Chem.* **2005**, *631*, *1272.*
(13) Höppe, H. A. *Solid State Sci.* **2005**, *7*, 1209.
(14) *SHELXTL X-Ray Single Crystal Analysis System*, version 5.1; Siemens Analytical X-Ray Instruments Inc.: Madison, WI, 1997.
(15) Petricek, V.; Dusek, M.; Palatinus, L. *Jana2000*; Institute of Physics: Praha, Czech Republic.

Table 2. Crystallographic Data of Ln(PO$_3$)$_3$ (Ln = Tb−Lu)

compd	space group	*a*/Å	*b*/Å	*c*/Å	*β*/deg	**q**
Tb(PO$_3$)$_3$	*Cc*(0*β*0)0	14.2242(19)	6.7252(13)	10.1236(16)	127.650(9)	0.364(2)**b***
Dy(PO$_3$)$_3$	*Cc*(0*β*0)0	14.174(4)	6.7095(14)	10.095(3)	127.62(2)	0.364(2)**b***
Ho(PO$_3$)$_3$	*Cc*(0*β*0)0	14.134(3)	6.6933(13)	10.064(2)	127.60(3)	0.361(2)**b***
Er(PO$_3$)$_3$	*Cc*(0*β*0)0	14.0543(16)	6.6585(11)	10.0018(12)	127.53(1)	0.362(2)**b***
Tm(PO$_3$)$_3$	*Cc*(0*β*0)0	14.0811(23)	6.6639(13)	10.0202(21)	127.68(1)	0.360(2)**b***
Yb(PO$_3$)$_3$	*Cc*(0*β*0)0	13.999(6)	6.6469(16)	9.959(5)	127.60(3)	0.361(2)**b***
Lu(PO$_3$)$_3$	*Cc*	13.972(1)	20.018(2)	9.9556(9)	127.351(6)	

Table 3. Atomic Coordinates and Isotropic Displacement Parameters U_{eq}/Å^2 for Dy(PO$_3$)$_3$ with Esd's in Parentheses

atom	*x*	*y*	*z*	U_{eq}[a]
Dy1	−0.4471	0.2490(4)	−0.247	0.0327(2)
P1	−0.2869(7)	0.8952(9)	−0.9010(8)	0.025(3)
P2	−0.1939(10)	0.5845(3)	−0.9998(15)	0.0324(15)
P3	−0.0974(7)	0.9022(10)	−0.0834(9)	0.032(3)
O12	−0.2402(12)	0.705(2)	−0.9203(16)	0.050(9)
O23	−0.1951(7)	0.733(2)	−0.1195(12)	0.025(4)
O31	−0.1659(14)	0.024(3)	−0.238(2)	0.102(11)
O101	−0.3640(12)	0.840(3)	−0.869(2)	0.052(9)
O102	−0.3247(15)	0.022(2)	−0.0373(19)	0.061(10)
O201	−0.0958(14)	0.470(2)	−0.894(2)	0.035(9)
O202	−0.3088(17)	0.487(3)	−0.1328(18)	0.093(9)
O301	−0.0604(15)	0.029(3)	−0.942(2)	0.069(11)
O302	0.0018(13)	0.822(2)	−0.091(2)	0.065(9)

[a] U_{eq} is defined as one-third of the trace of the $\mathbf{U}_{ij}$ tensor.

4000 cm^{-1}. The samples were thoroughly mixed with dried KBr (1 mg sample, 200 mg KBr). Raman spectra were excited by a Bruker FRA 106/S module with an Nd−YAG laser (λ = 1064 nm) scanning a range from 100 to 3500 cm^{-1}.

3. Crystal Structure of Ln(PO$_3$)$_3$ with Ln = Tb, Dy, Ho, Er, Tm, and Yb

The incommensurately modulated structure of the isotypic Ln(PO$_3$)$_3$ with Ln = Tb, Dy, Ho, Er, Tm, and Yb will be illustrated on the Dy compound. The Lu and Gd compound crystallize commensurately adopting normal superstructures and will be described in section 4.

For understanding the incommensurate modulation, it is generally useful to perform a superstructure refinement as an approximation of the incommensurate structure model. Since the modulation vector of Lu(PO$_3$)$_3$ is commensurate and very close to those found in Ln(PO$_3$)$_3$ (Ln = Tb−Yb), the in section 4 described crystal structure of Lu(PO$_3$)$_3$ represents this approximation.

Basic Structure. The crystal structure consists of infinite zigzag chains of PO$_4$ tetrahedra connected by common corners giving the polyphosphate anion PO$_3^-$. Between these chains the lanthanoid cations are positioned and coordinated by six terminal oxygen atoms forming a slightly distorted octahedron. Figure 2 illustrates the unit cell of the basic structure which could be refined only by applying distance and angle restraints in some cases. Additionally, exceedingly large anisotropic displacement parameters (ADPs) for most of the atoms were obtained. Especially the ADPs of the heavy atoms suggested how the positional modulation may interfere with the basic structure.

Modulated Structure of Ln(PO$_3$)$_3$ with Ln = Tb, Dy, Ho, Er, Tm, and Yb. Considering the satellite reflections which obey the modulation vector **q** = 0.364(2)**b*** (Figure 3) positional sinoidal modulation waves were initially introduced for the Dy atoms (Figure 4). The polyphosphate chains apparently respond to this modulation, and therefore, analogous modulation waves were introduced by applying soft restraints on bond lengths inside the phosphate chain. As a result, almost constant P−O distances (average distances: 157.2(9) pm for P−O^{br} and 145.7(8) pm for P−O^{term}) over the whole modulation period *t* were obtained (Figure 5). The Dy atoms are coordinated by terminal oxygen atoms only. Also, the Dy−O distances (average distance: 224.9(9) pm) and angles O−Dy−O vary in a rather close range giving an almost octahedral coordination sphere at every point of the modulation period (Figure 6). Consequently, the ADPs adopt reasonable values and give quite spherical ellipsoids for all atoms. The absence of an inversion center was proved by observation of the nonlinear optical SHG effect.

Crystallographic Classification. In former publications, the diffraction patterns were indexed on the basis of a monoclinic body-centered unit cell.[1] This is equivalent to the face-centered unit cell (standard unit cell setting) used herein. Also, our single-crystal data collections revealed besides a *C*-centering (reflections $h + k = 2n + 1$ are absent) a significant weakness of the reflections $h + l = 2n + 1$ and $k + l = 2n + 1$ indicating a pseudo-face-centering of the unit cell giving a rather poor signal-to-noise ratio of the data sets.

This observation can be understood by looking at group−subgroup relationships, and a closer look allows one to formally derive the crystal structure of the late lanthanoid polyphosphates from a fcc packing by successive symmetry reduction and hierarchical substitution (Figure 7). Finally, this consideration confirms the chosen space group of the basic structure, i.e., *Cc*. In the following treatment the oxygen atoms have been omitted. It is also useful to understand the close relationship of the structure of the incommensurately modulated phases with the commensurate phases.

Initially, the symmetry reduction starts with a fictitious fcc arrangement of Dy atoms adopting space group *Fm*3*m* (No. 225) descending via *F*4/*m* 2/*m* 2/*m* to an *F*-centered orthorhombic unit cell. Subsequent substitution of half of the Dy atoms by P gives a *C*-centered cell. Further reduction results in a monoclinic cell enabling the splitting of the P position resulting in two and, after loosing the inversion center, three crystallographically independent positions in *Cm* (No. 8). A final doubling of the *c*-axis and a following transformation according to crystallographic conventions allows the correct space group *Cc* (No. 9) of the basic structure to be obtained. The complete unit cell of the basic

Table 4. Anisotropic Displacement Parameters $U_{ij}/Å^2$ for the Atoms in $Dy(PO_3)_3$ with Esd's in Parantheses[a]

atom	U_{11}	U_{22}	U_{33}	U_{12}	U_{13}	U_{23}
Dy1	0.0293(2)	0.0352(3)	0.0382(3)	0.0029(4)	0.02294(19)	0.0047(3)
P1	0.019(3)	0.035(3)	0.012(2)	0.003(2)	0.006(2)	0.006(2)
P2	0.0384(17)	0.0240(14)	0.0455(15)	0.000(3)	0.0311(12)	0.001(4)
P3	0.028(3)	0.039(4)	0.029(3)	0.005(3)	0.018(2)	0.011(3)
O12	0.037(11)	0.054(9)	0.031(7)	0.028(7)	0.008(7)	0.002(5)
O23	0.015(4)	0.035(6)	0.024(4)	−0.006(5)	0.011(3)	−0.008(5)
O31	0.067(15)	0.123(11)	0.051(6)	−0.041(10)	0.003(9)	0.057(7)
O101	0.000(7)	0.127(15)	0.047(10)	0.002(7)	0.023(7)	0.024(9)
O102	0.082(11)	0.082(10)	0.052(9)	0.073(8)	0.058(9)	0.072(8)
O201	0.046(9)	0.031(7)	0.065(10)	0.032(6)	0.053(8)	0.044(7)
O202	0.067(10)	0.126(14)	0.028(6)	−0.026(9)	−0.001(6)	0.016(7)
O301	0.055(10)	0.086(13)	0.098(12)	0.023(8)	0.063(10)	0.011(9)
O302	0.059(9)	0.036(9)	0.064(8)	0.001(7)	0.018(7)	−0.003(7)

[a] The anisotropic displacement factor exponent is of the form $\exp\{-2\pi^2(U_{11}h^2a^{*2} + ... + 2U_{13}h|a^*c^*)\}$.

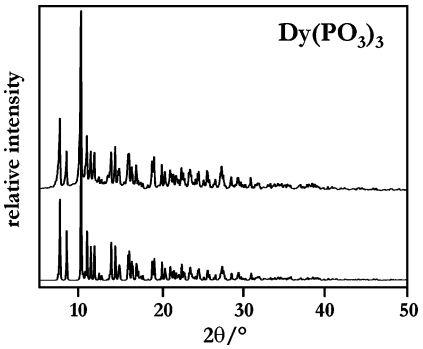

Figure 1. Comparison of a measured (above) and a calculated (below) powder diffraction pattern of $Dy(PO_3)_3$.

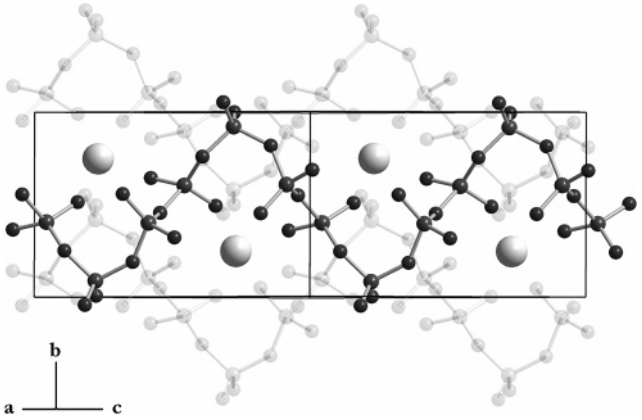

Figure 2. Representation of the basic structure. Two of the three phosphate chains are in the background (shadowed), and the Ln^{3+} ions are shown as large gray spheres.

structure is then obtained by a hierarchical substitution of the P atoms with the respective PO_4 tetrahedra.

4. Crystal Structures of $Lu(PO_3)_3$ and $Gd(PO_3)_3$

Crystal Structure of $Lu(PO_3)_3$. In $Lu(PO_3)_3$ no incommensurate modulation has been found, but a 3-fold superstructure along **b** (i.e., $\mathbf{q} = 1/3\mathbf{b}^*$) of the basic structure was located. The structure model was refined as a 3-fold superstructure of the basic unit cell in space group *Cc* (No. 9); the absence of an inversion center has been proved by a positive nonlinear optical SHG effect. The relevant crystallographic data and further details of the X-ray data collection are summarized in Table 5. In Table 6 selected interatomic distances and angles are listed. The principle of the superstructure is illustrated in Figure 8a. In $Lu(PO_3)_3$ the Lu atoms are coordinated 6-fold in an almost octahedral arrangement with Lu−O distances between 214 and 226 pm. The distances between bridging oxygen atoms and P lie between 153 and 161 pm, and for terminal oxygen atoms distances in the range from 145 to 148 pm to adjacent P atoms are found. All these bond lengths are in accordance with the sum of ionic radii of the respective ions.[16] The comparably large esd's of the distances reflect that the crystal structure of $Lu(PO_3)_3$ is close to an incommensurate disorder which cannot be resolved in the diffraction pattern. Therefore, soft restraints on the P−O distances have been applied. Other possible reasons for the large esd's like twinning could be excluded by a careful analysis of the whole data set and calculated precession photographs of the respective single crystal. Inversion twinning has been recognized and refined (Table 5).

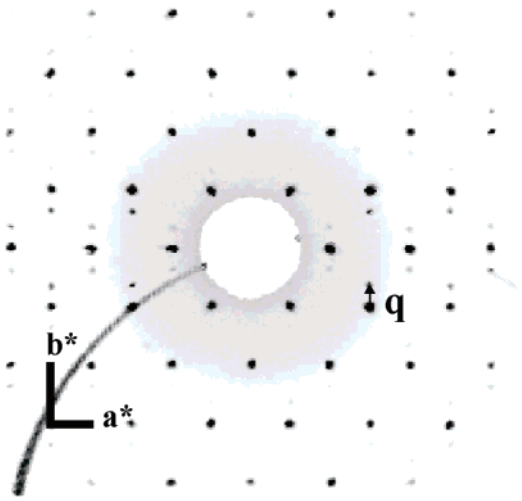

Figure 3. Representation of the reciprocal lattice layer (*hk*0) of $Dy(PO_3)_3$ calculated from IPDS data. The **q** vector and the axes **a*** and **b*** are indicated.

We performed a crystal structure refinement as a commensurately modulated structure of the basic unit cell with $\mathbf{q} = 1/3\mathbf{b}^*$. which led to reasonable results very close to those obtained by the previously mentioned superstructure refinement.

(16) Shannon, R. D.; Prewitt, C. T. *Acta Crystallogr. B* **1969**, *25*, 925.

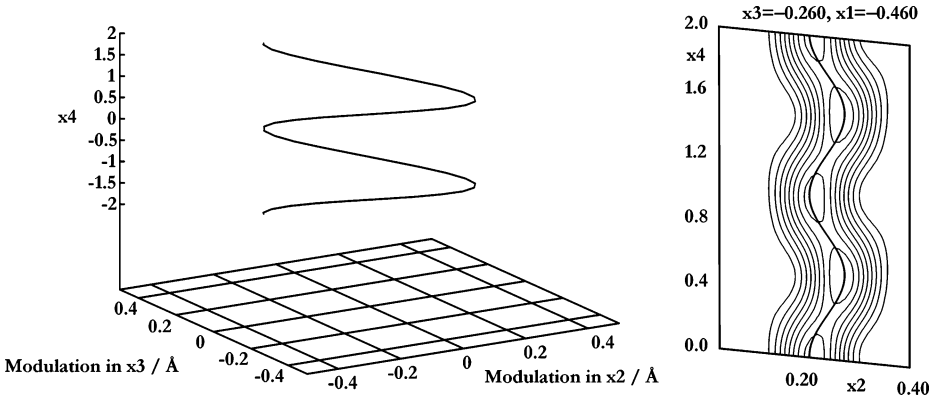

Figure 4. Dy modulation function (left) and F_o map showing the position modulation of Dy in Dy(PO$_3$)$_3$ (right).

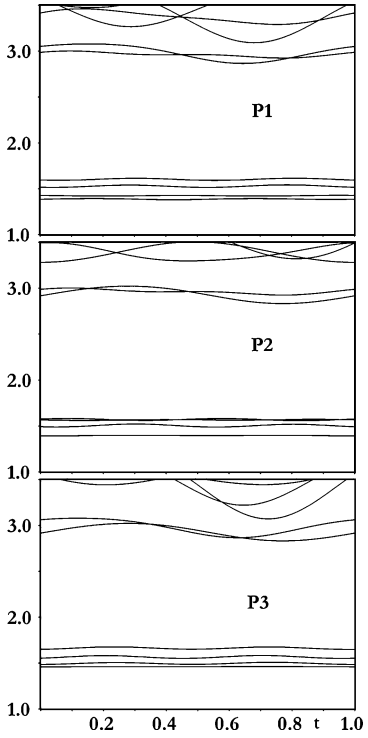

Figure 5. Coordination environment of the P atoms (distances in Å) against the modulation period *t*.

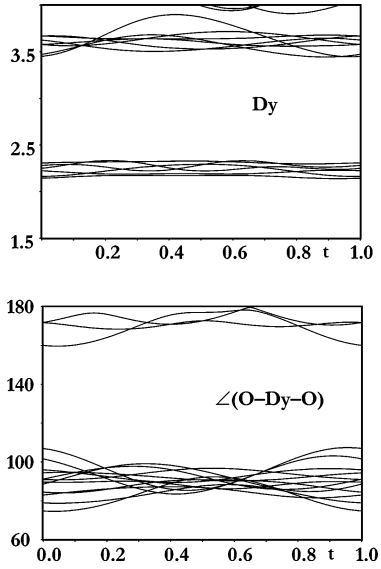

Figure 6. Dy coordination environment (top, distances in Å; bottom, O−Dy−O angles) against the modulation period *t*.

Since the modulation vector of Lu(PO$_3$)$_3$ is commensurate, the above-described superstructure refinement can be understood as an approximation of the incommensurate structure model of Ln(PO$_3$)$_3$ (Ln = Tb−Yb).

Crystal Structure of Gd(PO$_3$)$_3$. Like the crystal structure of previously mentioned Lu(PO$_3$)$_3$, the Gd compound is commensurate and can be derived from the basic structure of Dy(PO$_3$)$_3$. In contrast, the unit cell represents a 4-fold superstructure generating an inversion center which can be understood in terms of chemical twinning.[17,18] Therefore, Gd(PO$_3$)$_3$ adopts space group *I*2/*a* (No. 15). To clarify the relationship between the basic structure unit cell of the incommensurate phases and the crystal structure of Gd(PO$_3$)$_3$, the unconventional setting of space group *C*2/*c* was chosen. The relevant crystallographic data and further details of the X-ray data collection are summarized in Table 5. In Table 6 selected interatomic distances and angles are listed. The principle of the superstructure (doubling of the *a* and *b* axes of the basic unit cell) is illustrated in Figure 8c. In Gd(PO$_3$)$_3$ the heavy atoms are coordinated almost octahedrally with Gd−O distances between 224.7 and 233.1 pm. The distances between bridging oxygen atoms and P lie between 156.8 and 158.9 pm, and for terminal oxygen atoms distances in the range from 147.6 and 148.6 pm to adjacent P atoms are found. All these bond lengths are in accordance with the sum of ionic radii of the respective ions.[16]

5. Vibrational Spectroscopy

Figure 9 shows the IR and Raman spectra of Dy(PO$_3$)$_3$. The spectra of the other compounds are very similar. The IR spectra of *catena*-polyphosphates are not significantly different from those of *catena*-oligophosphates.[19] The only characteristic bands should be found in the region between 800 and 650 cm^{-1}, where the number of bands should correspond to the periodicity of the phosphate chain. This holds quite reliably only for low chain periodicities. In

(17) Andersson, S. *Angew. Chem., Int. Ed. Engl.* **1983**, *22*, 69.
(18) Höppe, H. A.; Kotzyba, G.; Pöttgen, R.; Schnick, W. *J. Mater. Chem.* **2001**, *11*, 3300.
(19) Rulmont, A.; Cahay, R.; Liegeois−Duyckaerts, M.; Tarte, P. *Eur. J. Solid State Inorg. Chem.* **1991**, *28*, 207.

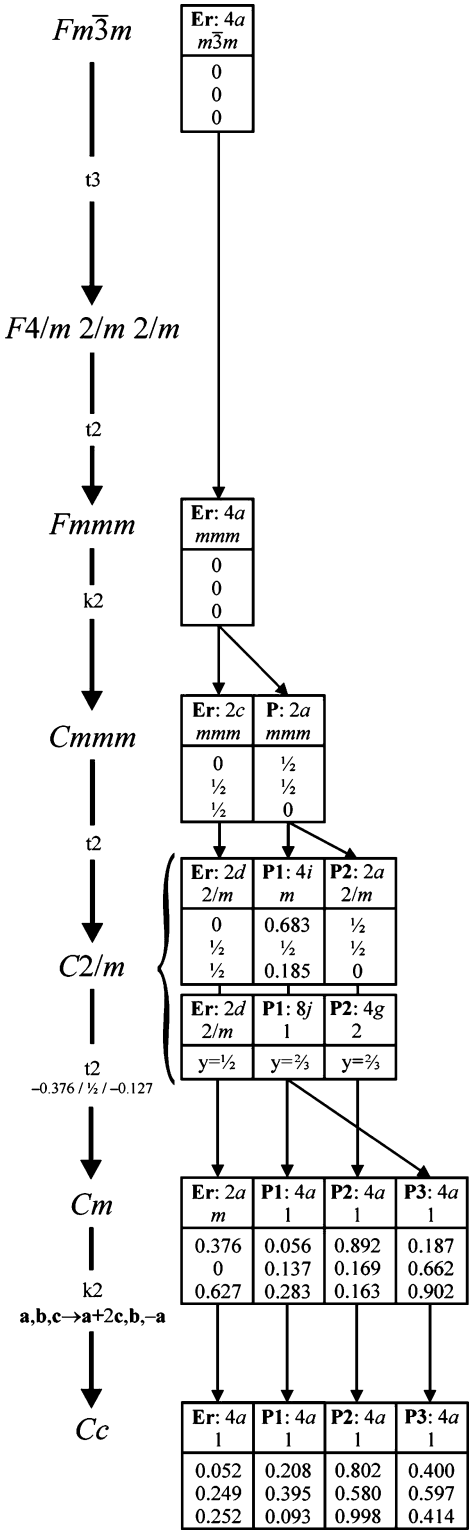

Figure 7. Group−subgroup relation scheme between the Ln−P substructure of $Ln(PO_3)_3$ and the fcc packing shown with Ln = Er.

$Dy(PO_3)_3$, the characteristic frequencies of *catena*-polyphosphate chains such as the $\nu_{as}(PO_2)$ are detected between 1200 and 1350 cm^{-1} with a maximum at 1252 cm^{-1}, the very intense ν_{as}(POP) at 946 cm^{-1} and $\nu(PO^{term})$ ranging from 980 up to 1100 cm^{-1}. Additionally, the Raman spectra of $Dy(PO_3)_3$ show strong vibrations in the region between 1190 and 1240 ($\nu_s(PO^{term})$) and at 680 cm^{-1} (ν_s(POP)). In the Raman spectrum of $Er(PO_3)_3$ exceedingly strong bands are found around 3000 cm^{-1} which can be assigned to an emission upon excitation by the Raman laser from the Er ground state (Figure 10). Thus, the observed vibrational data are in good agreement with expected values.[20]

Table 5. Crystallographic Data for $Gd(PO_3)_3$ and $Lu(PO_3)_3$ (Esd's in Parentheses)

Crystal Data

$Gd(PO_3)_3$	$F(000) = 2896$
$M_r = 394.17$	$\rho_{X-ray} = 3.388$ g cm^{-3}
monoclinic	Mo Kα radiatn
space group *I*2/*a* (No. 15)	$\lambda = 71.073$ pm
$a = 2601.7(2)$ pm	$\mu = 9.23$ mm^{-1}
$b = 1351.1(1)$ pm, $\beta = 119.311(6)°$	$T = 293(2)$ K
$c = 1008.4(1)$ pm	cryst shape: block
$V = 3091.0(3) \times 10^6$ pm^3	$0.03 \times 0.04 \times 0.04$ mm^3
$Z = 16$	colorless

Data Collection (Stoe IPDS-II)

abs corr: numerical	$h = -33 \rightarrow 33$
$T_{min} = 0.7223$; $T_{max} = 0.8441$	$k = -17 \rightarrow 17$
$R_{int} = 0.1147$	$l = -13 \rightarrow 13$
$2\theta_{max} = 55.0°$	3556 indpndnt reflcns
	2474 obsd reflcns ($F_o^2 \geq 2\sigma(F_o^2)$)

Refinement on F^2

R1 = 0.0386, wR2 = 0.0919, GooF = 0.890	$w^{-1} = \sigma^2F_o^2 + (0.0509P)^2$; $P = (F_o^2 + 2F_c^2)/3$
3556 reflcns	min resid electron density: −1.27 e Å^{-3}
237 params	max resid electron density: 1.69 e Å^{-3}

Crystal Data

$Lu(PO_3)_3$	$F(000) = 2256$
$M_r = 411.88$	$\rho_{X-ray} = 3.707$ g cm^{-3}
monoclinic	Mo Kα radiatn
space group *Cc* (No. 9)	$\lambda = 71.073$ pm
$a = 1397.2(1)$ pm	$\mu = 14.05$ mm^{-1}
$b = 2001.8(2)$ pm, $\beta = 127.351(6)°$	$T = 293(2)$ K
$c = 995.56(9)$ pm	Cryst shape: block
$V = 2213.5(3) \times 10^6$ pm^3	$0.05 \times 0.05 \times 0.06$ mm^3
$Z = 12$	colorless

Data Collection (Stoe IPDS-II)

abs corr: numerical	$h = -16 \rightarrow 16$
$T_{min} = 0.4512$; $T_{max} = 0.6827$	$k = -21 \rightarrow 23$
$R_{int} = 0.0833$	$l = -11 \rightarrow 11$
$2\theta_{max} = 55.0°$	5079 indpndnt reflcns
	3630 obsd reflcns ($F_o^2 \geq 2\sigma(F_o^2)$)

Refinement on F^2

R1 = 0.0417, wR2 = 0.0966, GooF = 0.898	$w^{-1} = \sigma^2F_o^2 + (0.0447P)^2$; $P = (F_o^2 + 2F_c^2)/3$
5079 reflcns	min resid electron density: −1.13 e Å^{-3}
312 params, 114 restraints	max resid electron density: 1.27 e Å^{-3}
Flack param: 0.49(3) (invers twin)	

Table 6. Selected Interatomic Distances/pm and Angles/deg in $Gd(PO_3)_3$ and $Lu(PO_3)_3$ with Esd's in Parentheses

param	$Gd(PO_3)_3$	$Lu(PO_3)_3$
$Ln1-O^{term}$	224.7(7)−233.1(7) (6 dists)	214.1(10)−223.6(12) (6 dists)
$Ln2-O^{term}$	225.0(7)−232.2(7) (6 dists)	218.6(12)−226.1(11) (6 dists)
$Ln3-O^{term}$		216.7(11)−221.4(14) (6 dists)
$P-O^{term}$	147.6(7)−148.6(7)	145.8(5)−147.5(5)
$P-O^{br}$	156.8(7)−158.9(7)	153.4(13)−161.0(17)
$O^{term}-P-O^{br}$	104.7(4)−111.6(5)	103.1(10)−114.8(10)
$O^{term}-P-O^{term}$	117.8(5)−119.3(6)	113.9(11)−121.6(9)
$O^{br}-P-O^{br}$	97.6(4)−106.6(6)	96.9(9)−106.4(11)
$P-O^{br}-P$	134.4(4)−141.3(5)	128.2(13)−150.8(12)

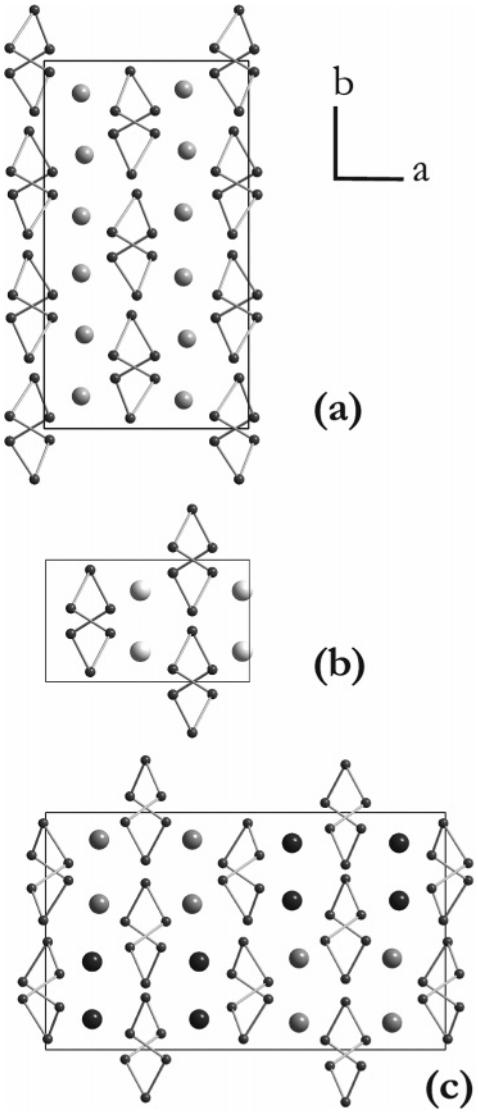

Figure 8. Illustration of the superstructure of (a) Lu(PO$_3$)$_3$ and (c) Gd(PO$_3$)$_3$ relatively to the (b) basic structure unit cell. The oxygen atoms have been omitted for clarity, and the phosphorus atoms have been connected by fictitious lines to visualize the connectivity of the tetrahedron centers.

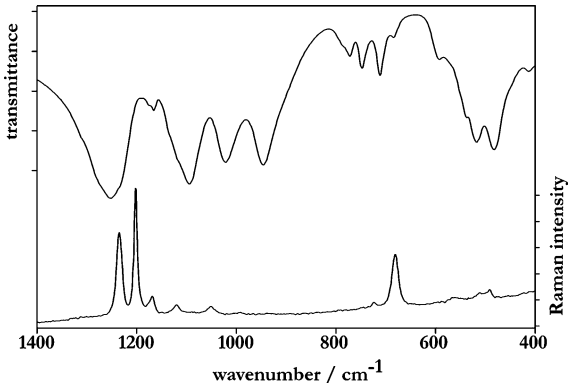

Figure 9. Infrared and Raman vibrational spectra of Dy(PO$_3$)$_3$.

6. Discussion and Conclusions

In this contribution, we shed light on inconsistencies in the literature and are able to present a consistent description of the crystal chemistry of the *catena*-polyphosphates of the late lanthanoids Ln(PO$_3$)$_3$ with Ln = Gd−Lu. During these investigations, a new synthesis method under reducing reaction conditions was successfully applied to obtain single-phase Tb(PO$_3$)$_3$.

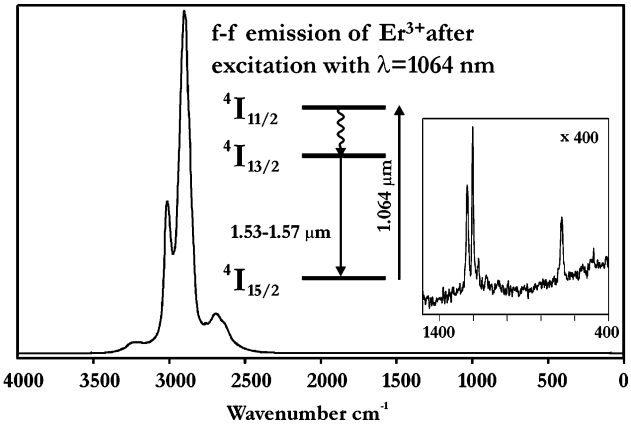

Figure 10. Raman spectrum of Er(PO$_3$)$_3$. The relevant electronic transition is indicated, the insert shows the respective Raman bands enlarged by a factor of 400.

Apparently, the preferred distances between the heavy atoms do not match with the periodicity of the polyphosphate chain and thus cause an incommensurate positional disorder of both the Ln^{3+} and the whole polyphosphate chain. To our knowledge the herein refined incommensurate crystal structures of polyphosphates are the first ones for this class of compounds. So far, only mono- or diphosphates like $K_3In(PO_4)_2$ and ZrP_2O_7 were found to show incommensurate crystal structures.[21,22]

Similar problems have been identified in transition metal and main group *C*-type phosphates $M^{III}(PO_3)_3$, but in these cases the structures could be described as 3-fold superstructures like in Cr(PO$_3$)$_3$ or Ga(PO$_3$)$_3$[23,24] and in one case as an 8-fold superstructure as in Ru(PO$_3$)$_3$.[25] Lu^{3+} is the smallest ion in the series described here, and accordingly Lu(PO$_3$)$_3$ can be assigned to the large group of *C*-type phosphates isotypic with Al(PO$_3$)$_3$,[26] while Gd(PO$_3$)$_3$, which contains the largest ion in this series, exhibits a novel structure type. Both termini of the series Ln(PO$_3$)$_3$ with Ln = Gd−Lu feature different strategies to avoid an incommensurate disorder probably depending on the size of the metal ions, i.e., the ions with half-filled and fully occupied 4f levels, respectively.

Moreover, we tried to elucidate the problem of pseudo-face-centering by identifying the on first sight not obvious close relationship between the fcc packing and the basic structure of the polyphosphates. This basic structure is obviously a versatile structural unit which is adopted by a large variety of trivalent metal ions, and this publication

(20) Ilieva, D.; Kovacheva, D. Petkov, Ch.; Bogachev, G. *J. Raman Spectrosc.* **2001**, *32*, 893.
(21) Arakcheeva, A.; Chapuis, G.; Petrícek, V.; Dusek, M.; Schönleber, A. *Acta Crystallogr. B* **2003**, *59*, 17.
(22) Withers, R. L.; Tabira, Y.; Evans, J. S. O.; King, I. J.; Sleight, A. W. *J. Solid State Chem.* **2001**, *157*, 186.
(23) Gruss, M.; Glaum, R. *Acta Crystallogr. C* **1996**, *52*, 2647.
(24) Anissimova, N.; Glaum, R. *Z. Anorg. Allg. Chem.* **1998**, *624*, 2029.
(25) Imoto, H.; Fukuoka, H.; Tsunesawa, S.; Horiuchi, H.; Amemiya, T.; Koga, N. *Inorg. Chem.* **1997**, *36*, 4172.
(26) van der Meer, H. *Acta Crystallogr. B* **1976**, *32*, 2423.

should contribute to the discussion why certain structural features are found in various compounds spread over the periodic system.

Further investigations to obtain detailed information about possible commensurate phases at lower or higher temperature and under high pressure and mechanisms thereto are in progress and will be reported elsewhere. Also the question how the electronic configuration of the Ln^{3+} may influence the crystal structure to become incommensurate will be addressed. A very interesting point currently under investigation is the question how the incommensurability may affect the optical properties of the lanthanoid ions, especially with regard to optical properties which are very sensitive to the coordination environment like quantum cutting[2] or possible application in upconversion materials.[3]

Acknowledgment. We thank Prof. Dr. H. Hillebrecht and Prof. Dr. C. Röhr, Albert-Ludwigs-Universität Freiburg, for valuable discussions and generous support. We also thank Prof. Dr. A. Seilmeier, Bayreuth University, for the nonlinear optical measurements and Mrs. A. Becherer, Albert-Ludwigs-Universität Freiburg, for measuring the vibrational spectra. Financial support by the Fonds der Chemischen Industrie (Liebig Habilitationsstipendium) is gratefully acknowledged.

Supporting Information Available: X-ray crystallographic files (CIFs) of the incommensurately modulated phase $Dy(PO_3)_3$ as well as of the commensurate phases $Gd(PO_3)_3$ and $Lu(PO_3)_3$. This material is available free of charge via the Internet at http://pubs.acs.org.

IC0616030